HAGO-Net: Hierarchical Geometric Massage Passing for Molecular Representation Learning

Hongbin Pei[1], Taile Chen[1], Chen A[1], Huiqi Deng[2], Jing Tao[1]*, Pinghui Wang[1], Xiaohong Guan[1]

[1]MOE KLINNS Lab, Xi'an Jiaotong University, China
[2]Shanghai Jiao Tong University, China
peihongbin@xjtu.edu.cn, stardust@stu.xjtu.edu.cn

Abstract

Molecular representation learning has emerged as a game-changer at the intersection of AI and chemistry, with great potential in applications such as drug design and materials discovery. A substantial obstacle in successfully applying molecular representation learning is the difficulty of *effectively* and *completely* characterizing and learning molecular geometry, which has not been well addressed to date. To overcome this challenge, we propose a novel framework that features a novel geometric graph, termed HAGO-Graph, and a specifically designed geometric graph learning model, HAGO-Net. In the framework, the foundation is HAGO-Graph, which enables a complete characterization of molecular geometry in a hierarchical manner. Specifically, we leverage the concept of n-body in physics to characterize geometric patterns at multiple spatial scales. We then specifically design a message passing scheme, HAGO-MPS, and implement the scheme as a geometric graph neural network, HAGO-Net, to effectively learn the representation of HAGO-Graph by horizontal and vertical aggregation. We further prove *D*HAGO-Net, the derivative function of HAGO-Net, is an equivariant model. The proposed models are validated by extensive comparisons on four challenging benchmarks. Notably, the models exhibited state-of-the-art performance in molecular chirality identification and property prediction, achieving state-of-the-art performance on five properties of QM9 dataset. The models also achieved competitive results on molecular dynamics prediction task.

Introduction

"Will AI redefine the future of chemistry?"— *Science* magazine raised this question in 125 cutting-edge scientific questions in 2021 (Sanders 2021). At an intersection of AI and chemistry, molecular representation learning has emerged as a game-changer, significantly reducing calculation time by five orders of magnitude compared to classical quantum methods, with an acceptable loss of accuracy (Gilmer et al. 2017). This remarkable improvement shows significant potential for various applications, including drug design and material discovery, drawing great attention from both computer science and chemistry (Bogojeski et al. 2020).

Nonetheless, a substantial obstacle in successfully applying molecular representation learning is the difficulty of *effectively* and *completely* characterizing and learning molecular geometry. Overcoming this challenge is essential because molecular geometry—the spatial arrangement of atoms within a molecule—has a strong direct relevance on molecular properties and dynamics from the perspective of quantum chemistry (Butler et al. 2018). To address this challenge, many powerful models have been proposed, such as DimeNet (Gasteiger, Gross, and Günnemann 2020), GemNet (Gasteiger, Becker, and Günnemann 2021), SphereNet (Liu et al. 2022), Equiformer (Liao and Smidt 2022). Although considerable progress has been made, the challenge has not been well addressed to date.

In order to effectively and completely learn molecular geometry, we present a novel framework, as illustrated in Fig. 1. The framework consists of two key steps: (1) **Complete characterization**, the framework features a novel geometric graph namely, the HAGO-Graph, to completely characterizes molecular geometry in a hierarchical manner; (2) **Effective representation learning**, the framework employs HAGO-Net, a specifically designed graph learning model, to effectively learn the invariant representation of HAGO-Graph, which serve as molecular representation. In addition, the derivative function of HAGO-Net, denoted as *D*HAGO-Net, is employed to learn equivariant representation. Finally, the obtained representations can be applied to molecular property and dynamics predictions, both of which are crucial in drug design and materials discovery.

Firstly, this framework is featured by its foundation, a novel **H**ier**A**rchical **GeO**metric Graph (HAGO-Graph), which hierarchically characterizes molecular geometry. *Adopting a hierarchical manner is motivated by the observation that molecular geometry is exhibited as patterns at multiple spatial scales*. As shown in Fig 2B, interatomic distances are exhibited at the atom scale, bond angles are observed at the atomic pair scale, dihedral angles are formed at the triplet scale, chirality is identified at the quintuplet scale, and higher-order geometry, *e.g.*, folding patterns (Moore et al. 2022) and curvature (Pei et al. 2020a), is displayed at larger spatial scales. In this way, any scale can be represented as one layer of the HAGO-Graph, *i.e.*, a subgraph, which is very flexible and have the capacity to achieve a complete characterization of molecular geometry.

*Corresponding Author

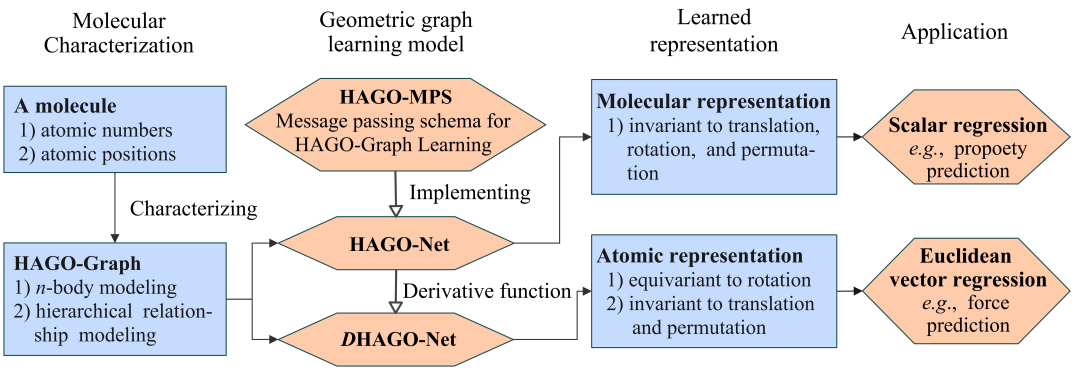

Figure 1: The proposed framework to characterize and learn molecular geometry. Molecular geometry is *completely* characterized as a HAGO-Graph and then *effectively* learned by the invariant HAGO-Net and equivariant *D*HAGO-Net. The learned molecular and atomic representation are then fed into various downstream applications, respectively.

Specifically, we leverage the concept of n-body in physics to characterize the geometric patterns at different scales. In a molecule, an n-body is a set of n neighboring atoms acting as a system, which is modeled as a node of the HAGO-Graph, as illustrated in Fig 2B and C. For instance, a 1-body node corresponds to an atom, and a 2-body node corresponds to an atomic pair. Based on the n-body modeling, we identify two types of geometry at each scale, intra-n-body geometry and inter-n-body geometry, which serve as node and edge attributes, respectively. We also define horizontal edges and vertical edges to connect the nodes and establish hierarchical structure of HAGO-Graph. In addition, we propose a novel geometric relationship, the relative orientation of tetrahedron (ROT), to identify molecular chirality. Notably, this capability is particularly valuable, as chirality plays a crucial role in determining molecular (bio)chemical properties. *Notable, the modeling of HAGO-Graph is general; molecular geometry at any spatial scale can be hierarchically characterized as intra-n-body and inter-n-body geometry, thereby achieving a complete characterization.*

Secondly, we propose **H**ier**A**rchical **GeO**metric **M**essage **P**assing **S**cheme (HAGO-MPS), a message passing scheme specifically designed to effectively learn representation of the proposed HAGO-Graph. HAGO-MPS incorporates two types of aggregation, as illustrated in Fig. 2C. One is vertical aggregation, which is employed to capture molecular geometry at a particular scale, while the other is horizontal aggregation, which exchanges information across different scales. In this way, the HAGO-MPS effectively captures and fuses molecular geometry at multiple scales.

Finally, we implement the HAGO-MPS as a **H**ier**A**rchical **GeO**metric graph neural **Net**work (HAGO-Net) by carefully designing basis functions and neural network modules in HAGO-MPS. The molecular representation learned by HAGO-Net is invariant to rigid transformations, since its input, the HAGO-Graph, is invariant. Furthermore, we prove the derivative function of HAGO-Net *w.r.t.* atomic positions, denoted as *D*HAGO-Net, can be used to learn atomic representation that is rotation equivariant and translation invariant and can be applied to Euclidean vector regression tasks, such as atomic force prediction. We empirically validate and analyze HAGO-Net and *D*HAGO-Net on four challenging molecular datasets, including MD17, QM9, GEOM-QM9, and PubChem3D. Notably, the proposed models exhibited state-of-the-art performance in molecular chirality identification and property prediction, achieving state-of-the-art performance on five properties of QM9 dataset. They also achieved competitive results in molecular dynamics prediction on MD17 dataset.

In summary, we propose a novel framework to learn molecular geometry, with four main contributions:

(i) We propose a novel geometric graph, HAGO-Graph, to completely characterize molecular geometry; in HAGO-Graph, we propose a novel chiral identity the ROT.

(ii) We design a message passing scheme, HAGO-MPS, to effectively learn representation of HAGO-Graph.

(iii) We implement HAGO-MPS as a graph neural network, HAGO-Net, and we further prove *D*HAGO-Net, the derivative function of HAGO-Net, is equivariant.

(iv) We validate and analyze HAGO-Net and *D*HAGO-Net by extensive comparisons on four benchmarks, and achieve state-of-the-art performance on property prediction.

Problem Definition

In this section, we introduce notations and formulate the problem of molecular representation learning. Consider a molecule with M atoms, denoted as $\mathcal{A} = \{a_i | i = 1, \ldots, M\}$, where a_i represents atom i. Each atom a_i is associated with an atomic number $z_i \in \mathcal{Z}$ and a spatial position in Cartesian coordinate system $\boldsymbol{p}_i \in \mathbb{R}^3$. The goal of molecular representation learning is to learn a representation vector $\boldsymbol{h}$ using a model $f(\mathcal{A}) \rightarrow \boldsymbol{h}$, and $\boldsymbol{h}$ is required to completely preserve geometric information in molecule $\mathcal{A}$, enabling its use in various downstream tasks off-the-shelf. In this paper, we take only atomic number and atomic position as inputs, while do not consider auxiliary features (*e.g.*, bond type and hybridisation type), as they are deemed non-essential from the perspective of quantum chemistry.

This paper focuses on two important tasks for molecular representation learning: scalar regression (*e.g.*, molecular

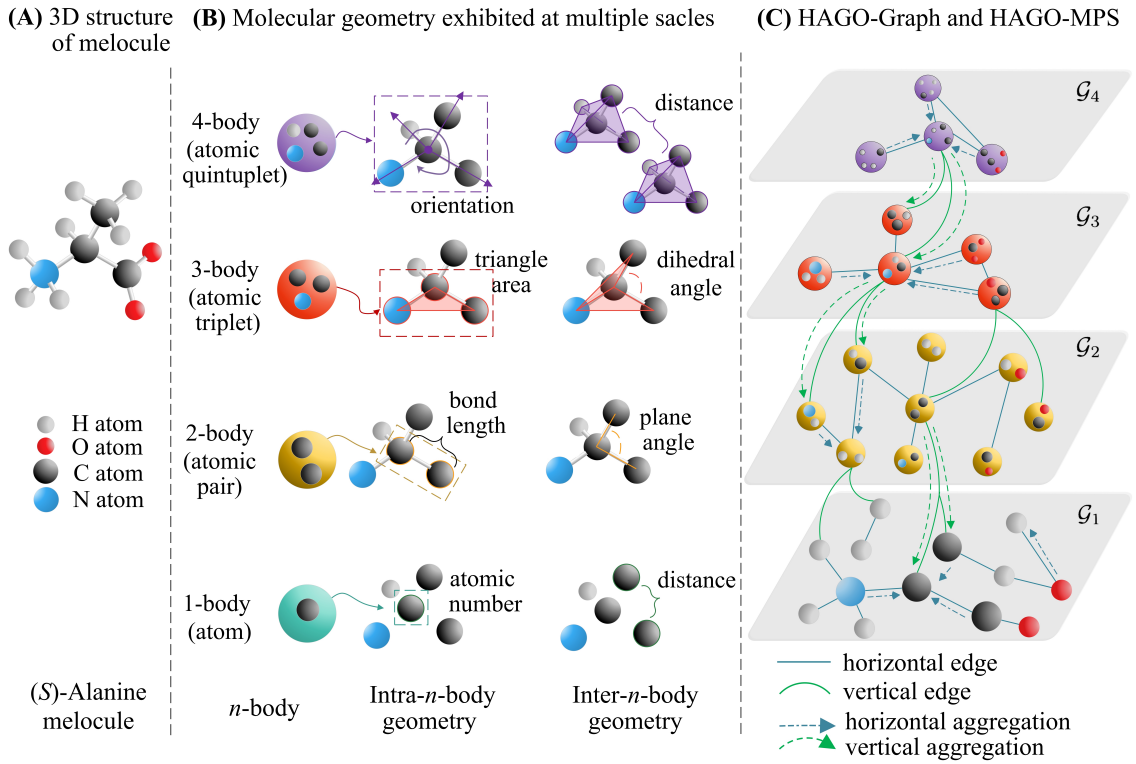

Figure 2: An illustration of molecular geometry, HAGO-Graph, and HAGO-MPS. (A) 3D structure of (S)-Alanine molecule. (B) An n-body is a set of neighboring atoms acting as a system, which is modeled as a node of the HAGO-Graph. Molecular geometry is exhibited as intra-n-body and inter-n-body geometry at four spatial scales. (C) HAGO-Graph $\mathcal{G}$ consists of 4 subgraphs $\mathcal{G}_1, \mathcal{G}_2, \mathcal{G}_3, \mathcal{G}_4$, in which horizontal edges connect nodes at a particular scale, vertical edges connect nodes to its descendants. HAGO-MPS performs messages passing through horizontal and vertical aggregation.

property prediction) and Euclidean vector regression (*e.g.*, atomic force prediction). To this end, there are two general requirements for the learned representation vector $\boldsymbol{h}$:

R1: **Invariance/Equivariance**. $\boldsymbol{h}$ is required to be invariant/equivariant for geometry-preserving mappings of $\mathcal{A}$, *i.e.*, isomorphisms of $\mathcal{A}$.

R2: **Discrimination**. $\boldsymbol{h}$ is required to completely encode molecular geometry of $\mathcal{A}$. As a result, $\boldsymbol{h}$ should be distinguishable between $\mathcal{A}$ and non-isomorphic $\mathcal{A}'$.

The **R1** aims to guarantee the learned representations of isomorphic molecules keep the "same". Specifically, equivariance refers to when the molecule $\mathcal{A}$ undergoes a isomorphism $\mathcal{T}$, such as permutation, translation, and rotation, its representation $\boldsymbol{h} = f(\mathcal{A})$ will undergo the same isomorphism as the molecule $\mathcal{A}$, *i.e.*, $f(\mathcal{T}(\mathcal{A})) = \mathcal{T}(f(\mathcal{A}))$. While invariance is a special case of equivariance, which requires that the representation $\boldsymbol{h} = f(\mathcal{A})$ stays unchanged to the isomorphism, *i.e.*, $f(\mathcal{T}(\mathcal{A})) = f(\mathcal{A})$. Generally, rotation equivariance is required for spatially-embedded tasks, such as force prediction, and invariance is required for molecule-level and scalar regression. The **R2** follows the basic principle of representation learning—*minimal sufficient statistic*, and aims to differentiate non-isomorphic molecules, especially to differentiate chiral molecules that are non-superposable mirror images of the original molecule.

Method

We start by presenting the geometric graph, HAGO-Graph, then describe the specifically designed message passing scheme, HAGO-MPS, and finally implement the HAGO-MPS as a graph neural network, HAGO-Net.

HAGO-Graph

In the proposed HAGO-Graph, we characterize molecular geometry in a hierarchical manner, to reflect different spatial scales of molecular geometry. We leverage the concept of n-body from physics to model these multiple scales. Specifically, we represent an n-body, *i.e.,* a set of n neighboring atoms acting as a system, as one node of the HAGO-Graph. For example, a 1-body node corresponds to an atom, while a 2-body node corresponds to an atomic pair. Consequently, the number n of atoms corresponds to a specific spatial scale of a molecule, and HAGO-Graph characterizes these multiple spatial scales by using n-bodies with diverse ns.

Based on the n-body modeling, we identify two types of geometry at each scale, intra-n-body geometry and inter-n-body geometry. The intra-n-body geometry is the geometry internal to an n-body node, *e.g.*, triangle area within a 3-body, while inter-n-body geometry describes the geometric relationship between two neighboring n-body nodes, *e.g.*, dihedral area formed by two 3-bodies. Taking the (S)-

Alanine molecule as an example, we illustrate its geometry in Fig. 2B. In HAGO-Graph, the intra-n-body and inter-n-body geometry is associated with nodes and edges, serving as node attributes and edge attributes, respectively. *It is worth noting that HAGO-Graph is general; one can incorporate any meaningful intra-n-body and inter-n-body geometry at any spatial scale, thereby achieving a complete characterization of molecular geometry.* The details of geometry used in our model are provided in (Git-repo 2023).

We define two types of edges, *horizontal edges* and *vertical edges*, to connect nodes and establish the hierarchical structure of HAGO-Graph. As shown in Fig. 2C, HAGO-Graph consists of several layers, *i.e.,* subgraphs. In a particular layer, the horizontal edge connects two neighboring nodes within a cutoff distance at the same spatial scale. For instance, at the 2-body scale, a horizontal edge connects two atomic pairs, and its edge attributes, *i.e.*, inter-2-body geometry, carry information about a plane angle. To link different layers, we define vertical edges to connect nodes to their descendant nodes in a lower layer, *i.e.*, to connect a n-body node to its descendant $(n-1)$-body nodes. A descendant node is a part of its parent node according to the atoms they contain. We define HAGO-Graph as follows.

Definition 1. Let $\mathcal{A} = \{a_i | i = 1, \ldots, M\}$ be a molecule with M atoms. A *hierarchical geometric graph* (HAGO-Graph) $\mathcal{G}$ for $\mathcal{A}$ is defined as N subgraphs connected hierarchically, $\mathcal{G} := \{\mathcal{G}_n | n = 1, \ldots, N\}$. Each subgraph $\mathcal{G}_n := \{\mathcal{V}_n, \mathcal{E}_n^-, \mathcal{E}_n^\perp\}$ characterizes geometry at scale n.
(1) $\mathcal{V}_n$ denotes the node set in which every node v is an n-body with n atoms. Let $v \in \mathcal{V}_n$ be a n-element subset of $\mathcal{A}$, *i.e.*, $v \subseteq \mathcal{A}$ and $|v| = n$, *e.g.*, node $v \in \mathcal{V}_2$ is an atomic pair.
(2) $\mathcal{E}_n^-$ contains horizontal edges, in which each horizontal edge $e_{v,u}^-$ is undirected and connects two neighboring nodes $v \in \mathcal{V}_n$ and $u \in \mathcal{V}_n$ of scale n within a cutoff distance.
(3) $\mathcal{E}_n^\perp$ contains vertical edges, in which each edge $e_{v,u}^\perp$ is directed and connects node $v \in \mathcal{V}_n$ to its descendant u. Node u is a descendant of node v, if $u \in \mathcal{V}_{n-1}$, and $u \subset v$.
(4) Node attribute $\boldsymbol{x}_v$ is associated with node $v \in \mathcal{V}_n$, describing the intra-n-body geometry of node v; edge attribute $\boldsymbol{x}_{u,v}$ is associated with the horizontal edge $e_{u,v}^- \in \mathcal{E}_n^-$, describing the inter-$n$-body geometry between the node v and u of scale n, *e.g.*, dihedral angle formed by two 3-bodies.

Relative Orientation of Tetrahedron for Identifying Molecular Chirality. We propose a novel geometric quantity, the relative orientation of tetrahedron (ROT), as an intra-4-body geometry in HAGO-Graph for identifying point chirality, which is a prevalent form of molecular chirality. Identifying molecular chirality is crucial, which is pivotal in determining molecular (bio)chemical properties. Let us first define chiral molecule and chiral identity.

Definition 2. (McNaught, Wilkinson et al. 1997). A molecule $\mathcal{A}$ is called *chiral* if it cannot be superimposed on its enantiomer (mirroring image) $\mathcal{A}'$ by any translations or rotations; otherwise is called *achiral*.

Definition 3. For a chiral molecule $\mathcal{A}$ and its enantiomer (mirroring image) $\mathcal{A}'$, a geometry quantity $\gamma \in \mathbb{R}$ is called *chiral identity* of enantiomers if it can differentiate $\mathcal{A}$ and $\mathcal{A}'$, *i.e.*, $\gamma(\mathcal{A}) \neq \gamma(\mathcal{A}')$.

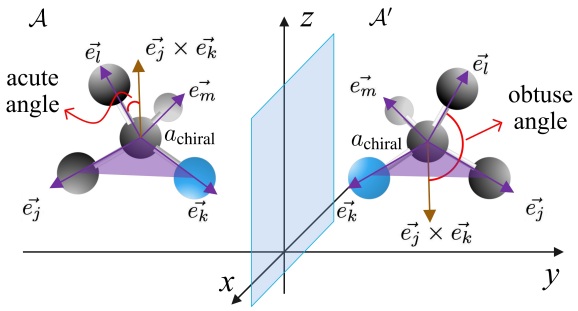

Figure 3: Illustration of the ROT for differentiating a chiral molecule $\mathcal{A}$ and its enantiomer (mirroring image) $\mathcal{A}'$. Theorem 4 proves that $\text{ROT}(\mathcal{A}) = -\text{ROT}(\mathcal{A}')$.

In order to identify molecular chirality, *i.e.*, to differentiate a chiral molecule $\mathcal{A}$ and its enantiomer $\mathcal{A}'$, we propose the ROT acting as the chiral identity, as illustrated in Fig. 3. Given a chiral atom, the ROT is calculated based on the 4-body most neighboring the chiral atom a_{chiral} as follow.

Step 1: Given molecule $\mathcal{A}$ and a chiral atom $a_{\text{chiral}} \in \mathcal{A}$, we choose the four atoms $\{a_j, a_k, a_l, a_m\}$ most neighboring the atom a_{chiral}. We calculate vectors from a_{chiral} to four neighboring atoms, $\vec{e_j}, \vec{e_k}, \vec{e_l}, \vec{e_m}$, by atomic position $\boldsymbol{p}$, *e.g.*, $\vec{e_j} = \boldsymbol{p}_j - \boldsymbol{p}_{chiral}$.

Step 2: We sort the four atoms according to their distances to a_{chiral} in descending order, and assume the sorted sequence is (a_j, a_k, a_l, a_m), without loss of generality.

Step 3: We compute the normal vector $\vec{n}$ of the plane spanned by vectors $\vec{e_j}$ and $\vec{e_k}$, by using a cross product operation, *i.e.,* $\vec{n} = \vec{e_j} \times \vec{e_k}$.

Step 4: The ROT is defined as the sign of the inner product of the normal vector $\vec{n}$ and the vector $\vec{e_l}$,

$$\text{ROT}(\mathcal{A}) = \text{sign}(\langle \vec{n}, \vec{e_l} \rangle) = \text{sign}(\langle \vec{e_j} \times \vec{e_k}, \vec{e_l} \rangle).$$

The ROT indicates whether the angle between $\vec{n}$ and $\vec{e_l}$ is acute or obtuse, as illustrated in Fig. 3. In fact, the normal vector $\vec{n}$ can be considered as the orientation of manifolds (Kreck 2013), which is based on the ordered cross product operation obeying the right-hand rule. Thus, the normal vector $\vec{n}$ will be inverted after mirroring, allowing it to distinguish chiral molecule $\mathcal{A}$ and its enantiomer $\mathcal{A}'$. Next, we prove the ROT is a chiral identity.

Theorem 4 (Proof in (Git-repo 2023))**.** *For a chiral molecule $\mathcal{A}$ and its enantiomer $\mathcal{A}'$, $\text{ROT}(\mathcal{A}) = -\text{ROT}(\mathcal{A}')$. In other words, the ROT is a chiral identity in Definition 3.*

Compared to ChIRo (Adams, Pattanaik, and Coley 2022), a deep model to learn chiral identity from data, the proposed ROT is much more *efficient* and *flexible* as it is a geometric feature, and it can be easily integrated in molecular models.

HAGO-MPS

Based on the HAGO-Graph, we propose HAGO-MPS, a message passing scheme specifically designed to effectively learn the representation of the HAGO-Graph. Neural message passing is a widely used solution for graph representation learning (Gilmer et al. 2017). In HAGO-MPS, we em-

ploy two types of aggregation strategies. The first is horizontal aggregation along horizontal edges, utilized to capture molecular geometry at a particular scale, whereas the second is vertical aggregation along vertical edges, which exchanges and fuses information across different scales.

Definition 5. *Hierarchical geometric message passing scheme* (HAGO-MPS) performs message passing on a HAGO-Graph $\mathcal{G}$ to learn node representations. Specifically, for a node $v \in \mathcal{V}_n$ at the n-th layer of $\mathcal{G}$, let $\boldsymbol{h}_v^{(k)}$ denote the representation vector of node v at k-th iteration. The initial representation is given as $\boldsymbol{h}_v^{(0)} = g(\boldsymbol{x}_v)$, where g is a geometric basis function. HAGO-MPS updates the representation $\boldsymbol{h}_v^{(k)}$ at the $(k+1)$-th iteration as follows,

$$\begin{aligned}
\boldsymbol{a}_v^{(k)} &= \rho_n^{(k)}(\{\boldsymbol{h}_v^{(k)}, \boldsymbol{h}_u^{(k)}, g(\boldsymbol{x}_{u,v}) | e_{u,v}^{-} \in \mathcal{E}_n^{-}\}) \\
\boldsymbol{b}_v^{(k)} &= \phi_n^{(k)}(\{\boldsymbol{h}_v^{(k)}, \boldsymbol{h}_u^{(k)} | e_{u,v}^{\perp} \in \mathcal{E}_n^{\perp}\}) \\
\boldsymbol{h}_v^{(k+1)} &= \tau_n^{(k)}(\boldsymbol{h}_v^{(k)}, \boldsymbol{a}_v^{(k)}, \boldsymbol{b}_v^{(k)}).
\end{aligned}$$

(i) $\rho_n^{(k)}$ is the function of horizontal aggregation, which aggregates messages along all horizontal edges $e_{u,v}^{-} \in \mathcal{E}_n^{-}$ associated with node v, *i.e.*, messages from all neighboring nodes in n-th layer. The inter-n-body geometry in the edge attribute $\boldsymbol{x}_{u,v}$ is integrated within these messages.
(ii) $\phi_n^{(k)}$ is the function of vertical aggregation, which propagates messages along all directed vertical edges $e_{u,v}^{\perp} \in \mathcal{E}^{\perp}$ associated with node v, *i.e.*, messages from all descendant nodes of node v in $n-1$-th layer. Vertical aggregation enables interaction between different scales.
(iii) $\tau_n^{(k)}$ is the function of fusion and transformation, which updates the representation vector of v by incorporating the two types of aggregated messages, $\boldsymbol{a}_v^{(k)}$ and $\boldsymbol{b}_v^{(k)}$.

The HAGO-MPS runs for K iterations. After K iterations, the representation vector of each 1-body node can be regarded as an atomic representation, *i.e.*, let $\boldsymbol{h}_v^{(K)}$ be $\boldsymbol{h}_{a_i}$, for $v \in \mathcal{V}_1$ and $v = a_i \in \mathcal{A}$. Moreover, the molecular representation $\boldsymbol{h}_{\mathcal{A}}$ can be easily acquired through a permutation-invariant pooling function that integrates all atomic representations, such as sum pooling,

$$\boldsymbol{h}_{\mathcal{A}} = \text{POOL}(\{\boldsymbol{h}_{a_i}\}) \quad \text{where } a_i \in \mathcal{A}.$$

Finally, the learned atomic and molecular representation can be fed into various downstream tasks.

HAGO-Net

We then implement HAGO-MPS as a **H**ier**A**rchical **GeO**metric graph neural **Net**work (HAGO-Net), so as to *effectively* learn the representation of HAGO-Graph. For message-passing neural networks (MPNNs), such as HAGO-Net, the Weisfeiler–Lehman (WL) test is a widely recognized approach to evaluating their expressive power to identify graph isomorphism. As proven in (Xu et al. 2018), if the aggregation functions and the graph-level pooling functions in an MPNN are injective (Pei et al. 2020b), the MPNN is as the same expressive power as the 1-WL test, which is sufficient for identifying nearly all graphs in practice, according to a recent empirical study (Zopf 2022).

We present HAGO-Net by carefully designing each module in HAGO-MPS, especially specifying geometric basis function g and aggregation functions $\rho_n^{(k)}$, $\phi_n^{(k)}$, $\tau_n^{(k)}$:
(i) For basis function g, we follow (Gasteiger, Gross, and Günnemann 2020) and set g as cubic basis function (CBF) or radial basis function (RBF), so as to transform geometric quantities x_v and $x_{u,v}$, *i.e.*, intra-n-body geometry and inter-n-body, to meaningful inputs for neural networks;
(ii) All aggregation functions, including functions $\rho_n^{(k)}$, $\phi_n^{(k)}$, $\tau_n^{(k)}$ for horizontal aggregation, vertical aggregation and fusion, consist of injective functions such as linear blocks, swish activation functions, Hadamard product, thereby making HAGO-Net as powerful as the 1-WL test.

The architecture of a typical n-body layer in HAGO-Net is illustrated in Appendix in (Git-repo 2023). Note that the proposed HAGO-Net is just an attempt. There may be more powerful architectures to implement HAGO-MPS with more basis functions, such as irreps features (Liao and Smidt 2022) and hyperbolic geometry (Wang et al. 2021).

Moreover, we prove the derivative function of HAGO-Net *w.r.t.* atomic positions, denoted as *D*HAGO-Net, is rotation equivariant and translation invariant. Thus, *D*HAGO-Net can be used to learn atomic representations that are applied to Euclidean vector regression tasks.

Lemma 6 (Proof in (Git-repo 2023))**.** *If an invariant function f takes positions as input, its derivative w.r.t. position is rotation equivariant and translation invariant.*

The Lemma 6 presents mathematical guarantee that the derivative function of the invariant model is translation invariant and rotation equivariant. *The lemma broadens the scope of numerous GCN-based invariant models, including HAGO-Net, to equivariant tasks*, such as force prediction in molecular dynamics simulation, as follows.

Theorem 7 (Proof in (Git-repo 2023))**.** *The DHAGO-Net is rotation equivariant and translation invariant.*

Experiments

In this section, we validate our models on benchmarks by answering the following three questions: **Q1**: Can the ROT distinguish enantiomers of chiral molecules? **Q2**: Can HAGO-Net predict molecular property effectively? **Q3**: Can *D*HAGO-Net predict molecular dynamics accurately? Model configurations in all experiments are detailed in our GitHub repository (Git-repo 2023).

We compare our models to 12 baselines, including SchNet (Schütt et al. 2017), sGDML (Chmiela et al. 2019), PhysNet (Unke and Meuwly 2019), DimeNet (Gasteiger, Gross, and Günnemann 2020), SEGNN (Brandstetter et al. 2021), PaiNN (Schütt, Unke, and Gastegger 2021), ComENet (Wang et al. 2022b), SphereNet (Liu et al. 2022), TorchMD (Thölke and De Fabritiis 2022), Equiformer (Liao and Smidt 2022), ChIRo (Adams, Pattanaik, and Coley 2022), and NequIP (Batzner et al. 2022). All experiments are conducted on eight NVIDIA Tesla V100 GPUs.

Task	Chirality identification	R/S classification for chiral center			
Model	**ROT** (our proposed geometric quantity)	SchNet	DimeNet	ChIRo	**HAGO-Net**
Accuracy (%)	96.5	54.5 ± 0.2	65.7 ± 2.9	$\underline{98.5 \pm 0.2}$	$\mathbf{98.9 \pm 0.2}$

Table 1: Accuracy of chirality identification on GEOM-QM9, and R/S classification on PubChem3D.

Method	μ	α	ϵ_{HOMO}	ϵ_{LUMO}	$\Delta\epsilon$	R^2	ZPVE	$U0$	U	H	G	c_v
SchNet	0.033	0.235	41.0	34.0	63.0	0.073	1.70	14.00	19.00	14.00	14.00	0.33
DimeNet	0.029	0.047	27.8	19.7	34.8	0.331	1.29	8.02	7.89	8.11	8.98	0.025
PhysNet	0.053	0.062	32.9	24.7	42.5	0.765	1.39	8.15	8.34	8.42	9.40	0.028
ComENet	0.024	0.045	23.1	19.8	32.4	0.259	**1.20**	6.59	6.82	6.86	7.98	0.024
SEGNN	$\underline{0.023}$	0.060	24.0	21.0	42.0	0.660	1.62	15.00	13.00	16.00	15.00	0.031
SphereNet	0.024	$\underline{0.045}$	22.8	19.6	31.1	0.268	1.26	6.31	6.36	$\underline{6.33}$	7.78	0.024
TorchMD	**0.011**	0.059	$\underline{20.0}$	$\underline{18.0}$	36.0	**0.033**	1.84	6.15	$\underline{6.38}$	**6.16**	$\underline{7.62}$	0.026
Equiformer	**0.011**	0.046	**15.0**	**14.0**	**30.0**	0.251	1.26	6.59	6.74	6.63	7.63	$\underline{0.023}$
HAGO-Net	0.023	**0.044**	22.6	19.1	$\underline{30.4}$	$\underline{0.230}$	$\underline{1.23}$	**5.89**	**6.11**	$\underline{6.33}$	**7.30**	**0.021**

Table 2: Comparisons between HAGO-Net and baselines in terms of MAE in property prediction on QM9 dataset.

Molecular Chirality Identification

We first evaluate the effectiveness of the proposed geometric quantity ROT in HAGO-Graph for chirality identification, *i.e.*, distinguishing a chiral molecule and its enantiomer, on the GEOM-QM9 dataset (Axelrod and Gomez-Bombarelli 2022). GEOM-QM9 includes 624 pairs of chiral molecules derived from QM9. By employing our proposed ROT, we successfully distinguish 602 out of 624 pairs, achieving an accuracy of 96.5% in Table 1, which suggests the ROT is effective. Notably, the calculation of rule-based ROT is very efficient, as it does not require learning from data.

We also evaluate HAGO-Net equipped with ROT on R/S classification, *i.e.*, classifying molecular chiral centers as clockwise (R) or counterclockwise (S). This experiment is conducted on a large dataset PubChem3D (Bolton et al. 2011), from which we use a subset with 78,000 enantiomers following the setup in ChIRo. HAGO-Net achieves the highest accuracy in R/S classification, as shown in Table 1. The best is shown in bold, and the second best is underlined.

Molecular Property Prediction

We evaluate the effectiveness of HAGO-Net in predicting molecular properties on QM9 dataset. QM9 is a benchmark that includes about 130,000 molecules, each associated with 12 molecular properties (Ruddigkeit et al. 2012). We adopt the same dataset split in (Liu et al. 2022), *i.e.*, 110,000 molecules for training, 10,000 molecules for validation, and the rest for testing. The evaluation metric is MAE between the ground-truth and the prediction for each property.

Table 2 summarizes the comparison results of property prediction. Our proposed HAGO-Net achieves the best performance on five properties and the second best performance on four properties. For the energy targets closely related to atoms, specifically U_0 (10.6% improvement), U (9.3% improvement), and G (4.3% improvement), our model shows outstanding performance. This may contributed by the fusion of geometry at multiple spatial scales. This suggests the ability of our model to learn high resolution information.

Molecular Dynamics Prediction

We evaluate the performance of *D*HAGO-Net in predicting molecular dynamics.The MD17 dataset contains the dynamics trajectories of energies and atomic forces of 8 organic molecules (Chmiela et al. 2017). We train a separate model for each molecule to predict atomic forces, using 1,000 samples for training and 1,000 samples for validation. This paper follows the experimental settings in (Liu et al. 2022), models are optimized using a joint loss function of energy and atomic forces, to ensure fitting conservative force, with only the force prediction performance being reported.

The comparison results of force prediction on MD17 dataset are summarized in Table 3. Our proposed *D*HAGO-Net achieve the best performance on three molecules and the second best performance on two molecules. In the case of aspirin, *D*HAGO-Net reduces prediction error by 25% compared to the competitors. Noting that we report the performance of NequIP in (Thölke and De Fabritiis 2022), the model has a updated version which achieves better results, but it requires much more spherical harmonics than ours.

Discussion

Comparisons to Related Works

Equivariant and Invariant Model. We briefly analyze existing works by categorizing them into two groups based on the geometry used as input. The first category is absolute position-based equivariant models, which directly take atomic absolute positions as input, *e.g.*, Cartesian coordinates, thereby incorporating geometry information of a molecule (Thomas et al. 2018; Brandstetter et al. 2022). These models require equivariance to transformations such as translation and rotation. To achieve this, they adopt equiv-

Method	Aspirin	Benzene	Ethanol	Malonaldehyde	Naphthalene	Salicylic acid	Toluene	Uracil
sGDML	29.5	8.7	14.3	17.8	4.8	12.2	6.1	10.4
SchNet	58.5	13.4	16.9	28.6	25.2	36.9	24.7	24.3
DimeNet	21.6	8.1	10.0	16.6	9.3	16.2	9.4	13.1
SphereNet	18.6	**7.7**	9.0	14.7	7.7	15.6	6.7	11.6
PaiNN	14.7	-	9.7	13.8	**3.4**	**8.5**	**4.1**	**6.0**
NequIP	15.1	8.1	9.0	14.6	4.2	10.3	4.4	7.5
***D*HAGO-Net**	**11.6**	8.0	**5.9**	**9.7**	5.8	8.7	6.5	9.3

Table 3: Comparisons between HAGO-Net and baselines in terms of MAE in force prediction on MD17 dataset.

ariant basis and activation functions, which limit their power to some extent and introduce high computational costs.

The second category is relative position-based invariant models, whose input is invariant geometric quantities that measure relative positions, such as bond angles, resulting in invariant models (Fang et al. 2022; Liu et al. 2022). in addition to efficiency, another advantage of invariant model is to easily integrate expert knowledge. Fundamentally, invariant models are based on an internal coordinate system using relative positions, *e.g.*, bond lengths, angles, and etc. In chemistry, the internal coordinate is frequently employed by experts because it is intuitive for human. For example, expert knowledge in molecular dynamics simulations is often expressed as constraints on bond lengths, bond angles, and torsions. These constraints are very easily implemented in invariant models with internal coordinates (Vaidehi and Jain 2015). In contrast, equivariant models have to characterize such constraints in Cartesian coordinates, which is non-intuitive and computationally expensive.

Our framework aligns with the principle of the invariant models because of the invariant geometric quantities adopted. The main challenge for invariant models is to completely characterize the molecular geometry because invariant geometry is usually defined in local, as cases demonstrated in (Joshi et al. 2023). Notably, *HAGO-Net addresses these challenge by hierarchically characterizing molecular geometry at multiple scales, thereby enabling a complete and multiple-resolution characterization.* This may break molecular representation bottleneck (Deng et al. 2022).

Hierarchy and n-Body Modeling. Many recent models adopt hierarchical molecular graph (Gao et al. 2023; Wang et al. 2022a), and n-body modeling(Shui and Karypis 2020; Qiao et al. 2022). In this paper, hierarchy and n-body modeling is motivated by our observation that molecular geometry exhibites at multiple spatial scales. As far as we are aware, this method is a novel contribution to 3D molecular learning.

In addition, a complete characterization of 3D molecular geometry is relatively straightforward. For a molecule of n atoms, there are $3n-6$ degrees of freedom. Mathmatically, any $3n-6$ independence geometric quantities can uniquely determine the molecule. The challenge is not just in completely characterizing molecular geometry, *but also in effectively preserving it into a representation vector by learning, which is the primary accomplishment of HAGO-Net.*

Computational Complexity Analysis

We give a computational complexity analysis for HAGO-Net, focusing on horizontal aggregation due to its significantly higher time complexity compared to other operations. Let M denote the number of atoms in a molecule and C denote the number of neighboring atoms within a cutoff distance. At a n-body layer, the complexity of horizontal aggregation for all nodes would be $O(M_nC_n)$, where M_n denotes the number of n-body nodes and C_n denotes the average number of neighbor nodes, $M_1 = M$, $C_1 = C$. The complexity can be further written as $O(\binom{C}{n}MC_n/n)$, because of $M_n = \binom{C}{n}M/n$. The complexity is mainly determined by C_n, because the other parameters are relatively small. By setting the cutoff distance as 5.0 Å, we have an average $C \approx 15$ for QM9 and an average $C \approx 12$ for MD17.

The complexity of HAGO-Net can be easily adjusted by changing C_n, which governs the spatial range within which horizontal aggregation is conducted. For instance, in experiments, we consider two atomic pairs to be neighboring if they have neighboring atoms, leading to $C_2 = C^2$ at 2-body layer. To control the complexity in 3-body layer, we only select the nodes with the top-2 smallest dihedral angle as the neighbor, *i.e.*, $C_3 = 2$. In summary, the complexity of HAGO-Net used in experiments is $O(\binom{C}{n}MC^2)$, which is comparable to that of SphereNet.

Conclusion

In this paper, we proposed a novel framework for *effectively* and *completely* characterizing and learning molecular geometry. The framework features a novel geometric graph, HAGO-Graph, and a specifically designed geometric graph learning model, HAGO-Net. By leveraging the concept of n-body, the framework is general and can incorporate meaningful molecular geometry at any spatial scales to achieve a complete characterization of molecular geometry. We validate the proposed framework through extensive comparisons on challenging benchmarks. The experimental results show the framework outperforms several powerful baselines.

In the future, we will further improve the HAGO-Net through adding self-attention mechanism among n-bodies (Wang et al. 2023), integrating domain knowledge (Liu et al. 2023), enhancing interpretability (Deng et al. 2023), and implementing optimal transport-based geometric aggregation (Chi et al. 2023), Bayesian uncertainty (Pei et al. 2022), and domain adaptation (Pang et al. 2022).

Acknowledgments

The authors would like to thank all the anonymous reviewers for their constructive comments. This work was supported by the National Natural Science Foundation of China under grant 62202369, U22B2019, 62372362, and Postdoctoral Innovative Talent Support Program of China (BX2021240).

References

Adams, K.; Pattanaik, L.; and Coley, C. W. 2022. Learning 3D Representations of Molecular Chirality with Invariance to Bond Rotations. In *International Conference on Learning Representations*.

Axelrod, S.; and Gomez-Bombarelli, R. 2022. GEOM: Energy-annotated molecular conformations for property prediction and molecular generation. arXiv:2006.05531.

Batzner, S.; Musaelian, A.; Sun, L.; Geiger, M.; Mailoa, J. P.; Kornbluth, M.; Molinari, N.; Smidt, T. E.; and Kozinsky, B. 2022. E (3)-equivariant graph neural networks for data-efficient and accurate interatomic potentials. *Nature communications*, 13(1): 1–11.

Bogojeski, M.; Vogt-Maranto, L.; Tuckerman, M. E.; Müller, K.-R.; and Burke, K. 2020. Quantum chemical accuracy from density functional approximations via machine learning. *Nature communications*, 11(1): 1–11.

Bolton, E.; Chen, J.; Kim, S.; Han, L.; He, S.; Shi, W.; Simonyan, V.; Sun, Y.; Thiessen, P.; Wang, J.; Yu, B.; Zhang, J.; and Bryant, S. 2011. PubChem3D: A new resource for scientists. *Journal of cheminformatics*, 3: 32.

Brandstetter, J.; Hesselink, R.; van der Pol, E.; Bekkers, E. J.; and Welling, M. 2021. Geometric and physical quantities improve e (3) equivariant message passing. *arXiv preprint arXiv:2110.02905*.

Brandstetter, J.; Hesselink, R.; van der Pol, E.; Bekkers, E. J.; and Welling, M. 2022. Geometric and Physical Quantities improve E(3) Equivariant Message Passing. In *International Conference on Learning Representations*.

Butler, K. T.; Davies, D. W.; Cartwright, H.; Isayev, O.; and Walsh, A. 2018. Machine learning for molecular and materials science. *Nature*, 559(7715): 547–555.

Chi, J.; Yang, Z.; Li, X.; Ouyang, J.; and Guan, R. 2023. Variational wasserstein barycenters with c-cyclical monotonicity regularization. In *Proceedings of the AAAI Conference on Artificial Intelligence*, volume 37, 7157–7165.

Chmiela, S.; Sauceda, H. E.; Poltavsky, I.; Müller, K.-R.; and Tkatchenko, A. 2019. sGDML: Constructing accurate and data efficient molecular force fields using machine learning. *Computer Physics Communications*.

Chmiela, S.; Tkatchenko, A.; Sauceda, H. E.; Poltavsky, I.; Schütt, K. T.; and Müller, K.-R. 2017. Machine learning of accurate energy-conserving molecular force fields. *Science Advances*, 3(5): e1603015.

Deng, H.; Ren, Q.; Zhang, H.; and Zhang, Q. 2022. Discovering and explaining the representation bottleneck of dnns. In *International Conference on Learning Representations*.

Deng, H.; Zou, N.; Du, M.; Chen, W.; Feng, G.; Yang, Z.; Li, Z.; and Zhang, Q. 2023. Understanding and unifying fourteen post-hoc attribution methods with taylor interactions. *arXiv preprint arXiv:2303.01506*.

Fang, X.; Liu, L.; Lei, J.; He, D.; Zhang, S.; Zhou, J.; Wang, F.; Wu, H.; and Wang, H. 2022. Geometry-enhanced molecular representation learning for property prediction. *Nature Machine Intelligence*, 4(2): 127–134.

Gao, Z.; Jiang, C.; Zhang, J.; Jiang, X.; Li, L.; Zhao, P.; Yang, H.; Huang, Y.; and Li, J. 2023. Hierarchical graph learning for protein–protein interaction. *Nature Communications*, 14(1): 1093.

Gasteiger, J.; Becker, F.; and Günnemann, S. 2021. Gemnet: Universal directional graph neural networks for molecules. In *Advances in Neural Information Processing Systems (NeurIPS)*, 6790–6802.

Gasteiger, J.; Gross, J.; and Günnemann, S. 2020. Directional message passing for molecular graphs. In *International Conference on Learning Representations (ICLR)*.

Gilmer, J.; Schoenholz, S. S.; Riley, P. F.; Vinyals, O.; and Dahl, G. E. 2017. Neural message passing for quantum chemistry. In *International conference on machine learning (ICML)*, 1263–1272.

Git-repo. 2023. https://github.com/XJTU-Graph-Intelligence-Lab/HAGO-Net/. Accessed: 2023-12-18.

Joshi, C. K.; Bodnar, C.; Mathis, S. V.; Cohen, T.; and Liò, P. 2023. On the expressive power of geometric graph neural networks. *arXiv preprint arXiv:2301.09308*.

Kreck, M. 2013. Orientation of Manifolds. *Bulletin of the Manifold Atlas–Definition*.

Liao, Y.-L.; and Smidt, T. 2022. Equiformer: Equivariant graph attention transformer for 3d atomistic graphs. *arXiv preprint arXiv:2206.11990*.

Liu, J.; Huang, Z.; Zhai, C.; and Liu, Q. 2023. Learning by Applying: A General Framework for Mathematical Reasoning via Enhancing Explicit Knowledge Learning. In *Thirty-Seventh AAAI Conference on Artificial Intelligence*.

Liu, Y.; Wang, L.; Liu, M.; Lin, Y.; Zhang, X.; Oztekin, B.; and Ji, S. 2022. Spherical message passing for 3d molecular graphs. In *International Conference on Learning Representations (ICLR)*.

McNaught, A. D.; Wilkinson, A.; et al. 1997. *Compendium of chemical terminology*, volume 1669. Blackwell Science Oxford.

Moore, P. B.; Hendrickson, W. A.; Henderson, R.; and Brunger, A. T. 2022. The protein-folding problem: Not yet solved. *Science*, 375(6580): 507–507.

Pang, M.; Wang, B.; Huang, S.; Cheung, Y.-M.; and Wen, B. 2022. A unified framework for bidirectional prototype learning from contaminated faces across heterogeneous domains. *IEEE Transactions on Information Forensics and Security*, 17: 1544–1557.

Pei, H.; Wei, B.; Chang, K.; Zhang, C.; and Yang, B. 2020a. Curvature regularization to prevent distortion in graph embedding. *Advances in Neural Information Processing Systems*, 33: 20779–20790.

Pei, H.; Wei, B.; Chang, K. C.-C.; Lei, Y.; and Yang, B. 2020b. Geom-GCN: Geometric Graph Convolutional Networks. In *International Conference on Learning Representations*.

Pei, H.; Yang, B.; Liu, J.; and Chang, K. C.-C. 2022. Active Surveillance via Group Sparse Bayesian Learning. *IEEE Transactions on Pattern Analysis and Machine Intelligence*, 44(3): 1133–1148.

Qiao, Z.; Christensen, A. S.; Welborn, M.; Manby, F. R.; Anandkumar, A.; and Miller III, T. F. 2022. Informing geometric deep learning with electronic interactions to accelerate quantum chemistry. *Proceedings of the National Academy of Sciences*, 119(31): e2205221119.

Ruddigkeit, L.; van Deursen, R.; Blum, L. C.; and Reymond, J.-L. 2012. Enumeration of 166 Billion Organic Small Molecules in the Chemical Universe Database GDB-17. *Journal of Chemical Information and Modeling*, 52(11): 2864–2875. PMID: 23088335.

Sanders, S. 2021. 125 questions: Exploration and Discovery. *Science/AAAS Custom Publishing Office: Washington, DC, USA*.

Schütt, K.; Kindermans, P.-J.; Sauceda Felix, H. E.; Chmiela, S.; Tkatchenko, A.; and Müller, K.-R. 2017. Schnet: A continuous-filter convolutional neural network for modeling quantum interactions. *Advances in neural information processing systems*, 30.

Schütt, K.; Unke, O.; and Gastegger, M. 2021. Equivariant message passing for the prediction of tensorial properties and molecular spectra. In *International Conference on Machine Learning*, 9377–9388. PMLR.

Shui, Z.; and Karypis, G. 2020. Heterogeneous molecular graph neural networks for predicting molecule properties. In *2020 IEEE International Conference on Data Mining (ICDM)*, 492–500. IEEE.

Thölke, P.; and De Fabritiis, G. 2022. Torchmd-net: equivariant transformers for neural network based molecular potentials. *arXiv preprint arXiv:2202.02541*.

Thomas, N.; Smidt, T.; Kearnes, S.; Yang, L.; Li, L.; Kohlhoff, K.; and Riley, P. 2018. Tensor field networks: Rotation-and translation-equivariant neural networks for 3d point clouds. *arXiv preprint arXiv:1802.08219*.

Unke, O. T.; and Meuwly, M. 2019. PhysNet: A neural network for predicting energies, forces, dipole moments, and partial charges. *Journal of chemical theory and computation*, 15(6): 3678–3693.

Vaidehi, N.; and Jain, A. 2015. Internal coordinate molecular dynamics: A foundation for multiscale dynamics. *The Journal of Physical Chemistry B*, 119(4): 1233–1242.

Wang, H.; Lian, D.; Tong, H.; Liu, Q.; Huang, Z.; and Chen, E. 2021. Hypersorec: Exploiting hyperbolic user and item representations with multiple aspects for social-aware recommendation. *ACM Transactions on Information Systems (TOIS)*, 40(2): 1–28.

Wang, L.; Liu, H.; Liu, Y.; Kurtin, J.; and Ji, S. 2022a. Learning hierarchical protein representations via complete 3d graph networks. In *The Eleventh International Conference on Learning Representations*.

Wang, L.; Liu, Y.; Lin, Y.; Liu, H.; and Ji, S. 2022b. ComENet: Towards complete and efficient message passing for 3D molecular graphs. *Advances in Neural Information Processing Systems*, 35: 650–664.

Wang, Y.; Li, S.; He, X.; Li, M.; Wang, Z.; Zheng, N.; Shao, B.; Liu, T.-Y.; and Wang, T. 2023. ViSNet: an equivariant geometry-enhanced graph neural network with vector-scalar interactive message passing for molecules. arXiv:2210.16518.

Xu, K.; Hu, W.; Leskovec, J.; and Jegelka, S. 2018. How powerful are graph neural networks? *arXiv preprint arXiv:1810.00826*.

Zopf, M. 2022. 1-WL Expressiveness Is (Almost) All You Need. *arXiv preprint arXiv:2202.10156*.